Chemical and Electrochemical Li-Insertion into the $Li_4Ti_5O_{12}$ Spinel

L. Aldon,*,† P. Kubiak,† M. Womes,† J. C. Jumas,† J. Olivier-Fourcade,† J. L. Tirado,‡ J. I. Corredor,‡ and C. Pérez Vicente‡

Laboratoire des Agrégats Moléculaires et Matériaux Inorganiques (UMR 5072 CNRS), Bât. 15, CC015, Université Montpellier II, Place Eugène Bataillon, 34095 Montpellier Cedex 5, France, and Laboratorio de Quimica Inorgánica, Facultad de Ciencias, Campus de Rabanales, Edificio C-3, 1 Planta, Universidad de Córdoba, 14071 Córdoba, Spain

Received July 9, 2004. Revised Manuscript Received September 29, 2004

Lithium has been inserted into the spinel $Li_4Ti_5O_{12}$ by both chemical and electrochemical methods. The cation distribution in the lithiated phases has been analyzed by ^{6,7}Li NMR, Raman spectroscopy, and X-ray diffraction, and the distribution in the chemically inserted compound has been analyzed additionally by neutron diffraction. A refinement of structural parameters has been carried out by applying the Rietveld method to the neutron diffraction pattern. It is shown that the two insertion methods are based on different mechanisms. Chemically inserted lithium ions are trapped in the (48f) sites of the spinel structure from which they cannot be extracted by electrochemical means. In contrast to the electrochemical Li-insertion, which is accompanied by a spinel to rocksalt phase transition, no such structural change is found for chemical insertion. The consequences of the two different mechanisms for the reversibility of the insertion process are discussed.

Introduction

Considerable efforts are currently being made in the search for new electrode materials suitable for use in advanced lithium accumulators. In the framework of this research, new negative electrode materials have to be developed working at a higher potential than the currently used carbon or graphite electrodes (∼1 V versus lithium) which are to be replaced for safety reasons.[1] Titanium oxides with the Ti^{4+}/Ti^{3+} redox couple working at approximately 1.5 V versus lithium fulfill this requirement. The spinel $Li_4Ti_5O_{12}$, a stable phase of the Li_2O-TiO_2 system, is a promising candidate because it allows insertion of 3 Li atoms per formula unit at a potential of 1.5 V.[2−10] The insertion mechanism is based on a spinel ↔ NaCl phase transition,[11,12] allowing the reduction of 3 Ti^{4+} atoms out of 5, which corresponds to a theoretical capacity of 175 Ah kg^{-1}.

Lithium can be introduced into the host lattice in two ways: (i) electrochemically, by using the material under study as one electrode in a test cell, allowing one to carry out charge/discharge cycles under conditions equal or similar to those in real batteries, and (ii) chemically, by immersing the material in a solution containing lithium. In this paper, we study the mechanisms governing the insertion processes of both methods. We focus on the structural changes inserted lithium causes in the host material and identify the lattice sites occupied by inserted lithium with the aim of a better understanding of the parameters determining the reversibility or irreversibility of the process. To this end, we used a number of different experimental techniques including X-ray and neutron diffraction, Raman spectroscopy, and ^{6,7}Li magic angle spinning nuclear magnetic resonance (MAS NMR).

Experimental Section

Synthesis. The starting spinel phase under study was obtained by a sol−gel route. Titanium isopropoxide $Ti(OiPr)_4$ was added to a solution of lithium acetate $Li(OAc)\cdot 2H_2O$ in ethanol to obtain the precursor gel. After solvent evaporation, the ground powder was dried in a Büchi oven at 110 °C for 24 h. The amorphous compound obtained at this stage was annealed at 800 °C in air for 8 h.

* Corresponding author. Phone: +33-476144548. Fax: +33-467143304. E-mail: aldon@iut-nimes.fr.
† Université Montpellier II.
‡ Universidad de Córdoba.

(1) Ferg, E.; Grummov, R. J.; De Kock, A.; Thackeray, M. M. *J. Electrochem. Soc.* **1994**, *141*, 147.
(2) Ozhuku, T.; Ueda, A.; Yamamoto, N. *J. Electrochem. Soc.* **1995**, *142*, 1431.
(3) Sarciaux, S.; Le Gal La Salle, A.; Guyomard, D.; Piffard, Y. *Mol. Cryst. Liq. Cryst.* **1998**.
(4) Pyun, S. I.; Kim, S. W.; Shin, H. C. *J. Power Sources* **1999**, *81−82*, 248.
(5) Zaghib, K.; Simoneau, M.; Armand, M.; Gauthier, M. *J. Power Sources* **1999**, *81−82*, 300.
(6) Jansen, A. N.; Kahaian, A. J.; Kepler, K. D.; Nelson, P. A.; Amine, K.; Dees, D. W.; Vissers, D. R.; Thackeray, M. M. *J. Power Sources* **1999**, *81−82*, 902.
(7) Bach, S.; Pereira-Ramos, J. P.; Baffier, N. *J. Power Sources* **1999**, *81−82*, 273.
(8) Prosini, P. P.; Mancini, R.; Petrucci, L.; Contini, V.; Villano, P. *Solid State Ionics* **2001**, *144*, 185.
(9) Ronci, F.; Reale, P.; Scrosati, B.; Rossi Albertini, V.; Perfietti, P.; Di Michiel, M.; Merino, J. M. *J. Phys. Chem. B* **2002**, *106*, 3082.
(10) Kubiak, P.; Garcia, A.; Womes, M.; Aldon, L.; Olivier-Fourcade, J.; Lippens, P. E.; Jumas, J. C. *J. Power Sources* **2003**, *119−121*, 626.
(11) Scharner, S.; Weppner, W.; Schmid-Beurmann, P. *J. Electrochem. Soc.* **1999**, *146*, 857.
(12) Panero, S.; Reale, P.; Ronci, F.; Rossi Albertini, V.; Scrosati, B. *Ionics* **2000**, *6*, 461.

10.1021/cm0488837 CCC: $27.50
Published on Web 12/04/2004

Methods of Characterization. X-ray diffraction showed the reaction product to be $Li_4Ti_5O_{12}$ containing TiO_2 (rutile) as an impurity. Manual grinding was performed in lithium acetate whose quantity was adjusted for complete elimination of the r-TiO_2 phase, after checking by X-ray diffraction. Firing at 900 °C for 72 h gave a pure and well-crystallized $Li_4Ti_5O_{12}$ compound.

Lithium inserted samples were prepared by both (a) electrochemical and (b) chemical routes.

Electrochemical Li-insertion was carried out in two-electrode Swagelock using Li and the spinel phase as electrodes and 1 M $LiPF_6$ (PC-EC-DMC 1:1:3) as electrolyte. The electrodes were prepared as 7 mm diameter pellets by pressing a mixture of 80% $Li_4Ti_5O_{12}$, 10% PVDF binder, and 10% carbon black to improve the mechanical and electronic conduction properties. WhatmanTM porous glass-paper disks supported the electrolyte solution. The cells were assembled inside an argon-filled glovebox. The electrochemical charge/discharge curves were recorded on a multichannel Mac Pile system under galvanostatic conditions at a *C*/15 rate; that is, a molar ratio Li/$Li_4Ti_5O_{12}$ equal to 1 was reached in 5 h. Under these conditions, 2.8 Li toms were inserted into $Li_4Ti_5O_{12}$, leading to the formula $Li_{6.8}Ti_5O_{12}$ and giving a reversible capacity of 154 Ah kg^{-1}. The black product obtained after Li-insertion becomes white after exposure in air for a few minutes.

Chemical insertion was carried out by immersing the powder sample for 24 h in solutions of *n*-butyllithium, (*n*-C_4H_9)Li, in hexane.[13] A thermostatic bath kept the temperature of the solution constant at 35 °C. The experimental device was kept under a dry argon atmosphere during the reaction. Chemical insertion gave a compound of composition $Li_{5.9}Ti_5O_{12}$. The chemical insertion process allows one to obtain the large amounts of sample (~10 g) required for the neutron diffraction experiments. The stability of this phase is high because the black color is still present after exposure in air for several weeks.

Sample Stoichiometry. The amount of inserted lithium was determined by atomic emission spectroscopy in an inductively coupled plasma on a Jobin Yvon JY24 spectrophotometer.

Raman Spectroscopy. Samples used for Raman spectroscopy were sealed in 1 mm glass capillaries. Spectra were recorded on a Dilor spectrometer using the green line (514.5 nm) of a Spectra Physics argon laser. The intensity of the incident light was kept below 140 mW.

X-ray Diffraction. X-ray diffractograms were recorded on a conventional Philips $\theta-2\theta$ diffractometer using Cu Kα radiation (1.5418 Å) and a nickel filter. Measurements on the electrochemically inserted phases were carried out under vacuum to avoid undesired reactions with air.

Neutron Diffraction. Neutron diffraction patterns were recorded at room temperature on the D1B diffractometer of the Institute Laue-Langevin (ILL, Grenoble, France) with a wavelength of 1.28 Å, between 10° and 90° 2θ, with a 0.02° 2θ step width and a data acquisition time of 8 h for each sample. The Rietveld analyses were carried out with the DBWS-9006 program developed by Wiles and Young.[14]

^{6,7}Li MAS NMR. ^{6,7}Li MAS NMR spectra were recorded at room temperature on a Bruker ACP-400 spectrometer in a magnetic field of 9.4 T. The powder samples were transferred to zirconia rotors, which were sealed in a glovebox under inert atmosphere. For ^{7}Li, the spectra were obtained by means of single pulses and a solid (quadrupolar) spin−echo sequence ($\pi/2-\tau-\pi/2-\tau$ acquisition, 8 μs pulses, and 2 s recycle delay). Typically, 500 scans were collected for each sample, using a spinning speed of 5.5 kHz at the resonance frequency of 155.5 MHz. For ^{6}Li, the resonance frequency was 58.9 MHz. The chemical shifts are given with respect to an aqueous LiCl solution.

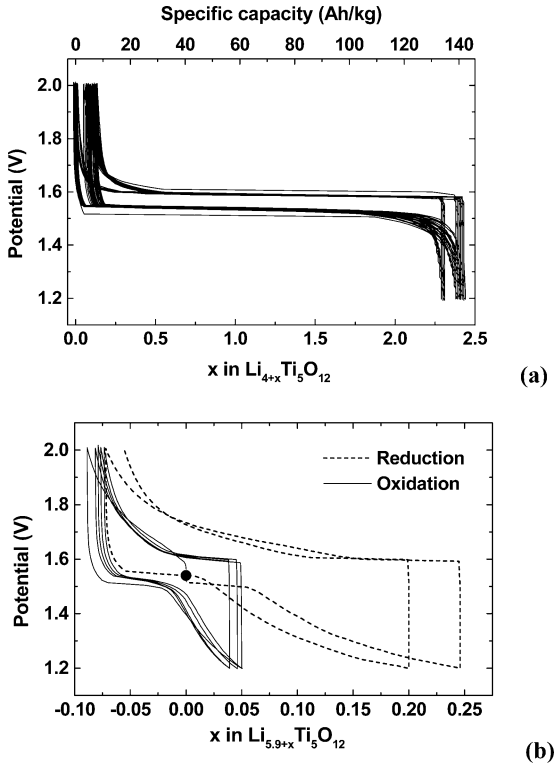

Figure 1. Electrochemical performances of $Li_4Ti_5O_{12}$ before chemical lithium-insertion (a), and after chemical Li-insertion given the $Li_{5.9}Ti_5O_{12}$ compound (b).

Results

The results described in the following are intended to elucidate the basic mechanisms of chemical and electrochemical lithium-insertion in the spinel $Li_4Ti_5O_{12}$. A first and very simple experiment indicating that the two insertion processes are based on different mechanisms consists of exposing the samples to air. While the pristine material is white, both lithiated samples are black, comparable to other compounds containing Ti^{3+}, such as Ti_2O_3 or the spinel $LiTi_2O_4$. Contact with air makes the electrochemically lithiated sample become white while the chemically lithiated compound conserves its black color, indicating a rapid reoxidation of Ti^{3+} to Ti^{4+} in the former and a more stable +3 oxidation state in the latter.

Further differences are found when both materials are subjected to electrochemical tests. Figure 1a shows the electrochemical properties of pristine $Li_4Ti_5O_{12}$. The discharge curve is characterized by a plateau at 1.55 V versus Li. Charge/discharge processes taking place on a constant potential are characteristic of a two-phase mechanism, where cycling is reversible between a Li-rich and a Li-poor phase. In the case of $Li_4Ti_5O_{12}$, the occurrence of a plateau has been attributed to a spinel to rocksalt phase transition, which is completed when a stoichiometry of $Li_7Ti_5O_{12}$ is reached. With a composition of $Li_{6.8}Ti_5O_{12}$ at the end of the discharge run, we effectively come very close to this theoretical limit by electrochemical insertion. Moreover, the insertion mechanism is highly reversible, as can be seen from Figure 1a, allowing electrochemical lithium extraction from $Li_{6.8}Ti_5O_{12}$. The behavior of the chemically inserted compound $Li_{5.9}Ti_5O_{12}$ is completely different. Figure 1b shows that, in the conditions of the experiment (dis-

(13) Thackeray, M. M.; David, W. I. F.; Goodenough, J. B. *Mater. Res. Bull.* **1982**, *17*, 785.
(14) Wiles, D. B.; Young, R. A. *J. Appl. Crystallogr.* **1995**, *28*, 366.

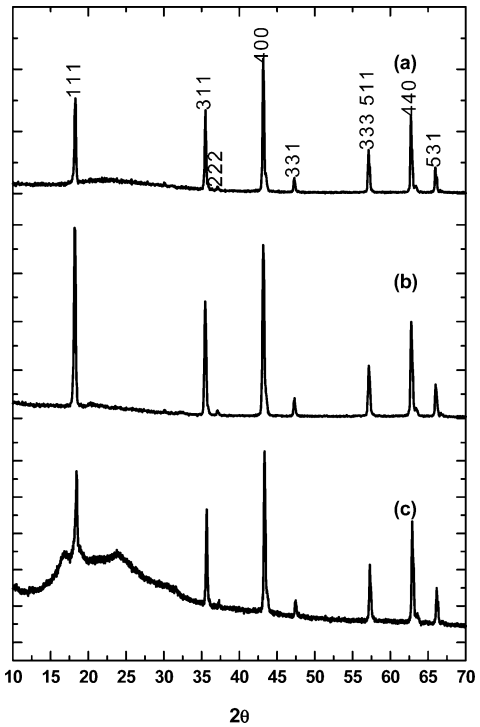

Figure 2. Experimental X-ray diffraction patterns of the pristine $Li_4Ti_5O_{12}$ (a), the chemically inserted $Li_{5.9}Ti_5O_{12}$ (b), and the electrochemically inserted $Li_{6.8}Ti_5O_{12}$ (c).

charge limited to 1.2 V, charge limited to 2 V), it is impossible to extract chemically inserted lithium by electrochemical means in this limited potential window. It is also impossible to insert further lithium and to reach the stoichiometry $Li_{6.8}Ti_5O_{12}$ obtained electrochemically when starting from the pristine material. These results suggest that chemically and electrochemically inserted lithium occupy different lattice sites in the spinel structure. A study by X-ray diffraction has therefore been carried out.

The X-ray diffraction (XRD) pattern of the white $Li_4Ti_5O_{12}$ powder sample obtained after impurity elimination is shown in Figure 2a. All of the reflections have been indexed in the *Fd*3*m* space group of the cubic spinel structure with a unit cell dimension of 8.3764 Å, which is in agreement with previously reported values.[15] No significant variations in the intensities of the peaks were observed for the black chemically inserted $Li_{5.9}Ti_5O_{12}$ compound shown in Figure 1b. Figure 1c shows the XRD pattern of the black electrochemically inserted $Li_{6.8}Ti_5O_{12}$ compound. The differences between X-ray diffraction patterns are still subtle. Thus, a neutron diffraction experiment was carried out to locate more precisely Li atoms in the structures.

Figure 3 shows the neutron diffraction patterns of the phases obtained before and after chemical insertion of Li together with calculated diffractograms obtained by Rietveld analysis. Slight variations in relative line intensities are observed between the pristine and the lithiated material. In the case of the chemically inserted phase, the global intensity of the neutron diffraction patterns was smaller by a factor of about 5, for the same counting time and sample holder filling. The results of

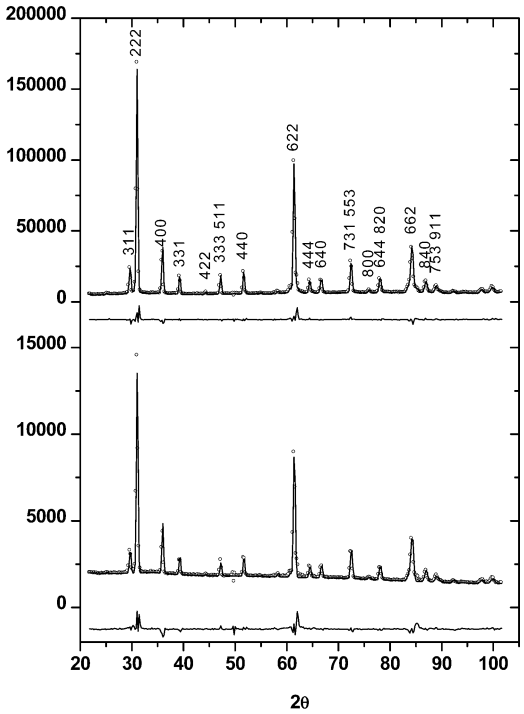

Figure 3. Experimental neutron diffraction patterns of both $Li_4Ti_5O_{12}$ and chemically inserted $Li_{5.9}Ti_5O_{12}$.

the Rietveld analysis are given in Table 1. The line intensities of the starting material agree well with the cation distribution $(Li)_{8a}[Li_{0.33}Ti_{1.66}]_{16d}O_4$ usually ascribed to this compound. In the case of the lithiated phase, the best agreement between experiment and simulation is obtained by supposing a partial filling by lithium of the octahedral 16c and the tetrahedral 48f sites, which remain unoccupied in the spinel structure.

^{6,7}Li MAS NMR was carried out to confirm this hypothesis. ^{7}Li MAS NMR single pulse and solid echospin yielded larger intensities but a poorer resolution, as compared to ^{6}Li spectra. Thus, in Figure 4, only the ^{6}Li spectra are shown. Both pristine ($Li_4Ti_5O_{12}$) and chemically lithiated ($Li_{5.9}Ti_5O_{12}$) samples show two signals. The lower intensity signal (shaded contribution in Figure 4) occurs at an upfield position (ca. −1 ppm) and can be ascribed in a first approach to octahedrally coordinated lithium. The second signal close to 0 ppm is ascribable to lithium in LiO_4 tetrahedra, as was previously reported for the $Li_4Ti_5O_{12}$ spinel.[16]

Due to the larger intensity and lower background noise, the quantification of the spectra was carried out on the ^{7}Li MAS NMR data, including up to three subspectra. Selected numerical results are presented in Table 2. Concerning the pristine compound $Li_4Ti_5O_{12}$, the relative integration of the signals gave 76% of total contribution for tetrahedral Li and 24% for octahedral Li, in good agreement with the expected Li distribution in both sites, that is, 75% in tetrahedral 8a sites and 25% in octahedral 16d sites (see Table 1). Concerning the lithiated phase, $Li_{5.9}Ti_5O_{12}$, the integration gave 70.2% and 29.8% for tetrahedral and octahedral Li, respectively. These values are very close of those obtained from the refinement of the neutron diffraction pattern (69.2% and 30.8%, see Table 1), thus confirming

(15) Deschanvres, A.; Raveau, B.; Sekkal, Z. *Mater. Res. Bull.* **1971**, *6*, 699.

(16) Kartha, J. P.; Tunstall, D. P.; Irvine, J. T. S. *J. Solid State Chem.* **2000**, *152*, 397.

Table 1. Selected Results of Rietveld Analyses of Neutron Diffraction Data for $Li_4Ti_5O_{12}$ and $Li_{5.9}Ti_5O_{12}$[a]

site	atom	x	y	z	B	occupancy
		$Li_4Ti_5O_{12}$: $a = 8.3764(4)$ Å, $R_{Bragg} = 3.1$, $S = 1.42$				
8a	Li	1/8	1/8	1/8	1.78(36)[a]	1[b]
16d	Li	1/2	1/2	1/2	1.78(36)[a]	0.1667[b]
	Ti				0.88(11)	0.8333[b]
32e	O	0.264(1)	0.264(1)	0.264(1)	0.98(5)	1[b]
		$Li_{5.9}Ti_5O_{12}$: $a = 8.3733(4)$ Å, $R_{Bragg} = 2.7$, $S = 1.31$				
8a	Li	1/8	1/8	1/8	1.37(6)[a]	0.71(2)
16c	Li	0	0	0	1.25(6)[a]	0.12(1)
16d	Li	1/2	1/2	1/2	1.25(6)[a]	0.1667[b]
	Ti				0.85(12)	0.8333[b]
32e	O	0.262(2)	0.262(2)	0.262(2)	0.80(2)	1[b]
48f	Li	0.374(2)	1/8	1/8	1.37(6)[a]	0.107(8)

[a] Space group: $Fd\bar{3}m$. Origin 2: 8a (1/8, 1/8, 1/8), 16c (0, 0, 0), 16d (1/2, 1/2, 1/2), 32e (x, x, x), 48f (x, 1/8, 1/8). [b] Fixed parameter. [c] Constraint to be equal.

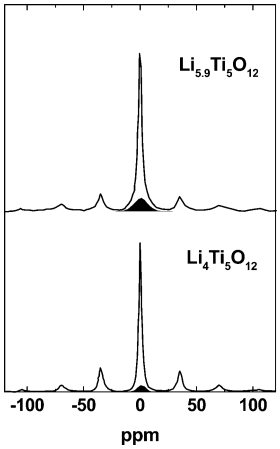

Figure 4. ^6Li MAS NMR spectra of both $Li_4Ti_5O_{12}$ and chemically inserted $Li_{5.9}Ti_5O_{12}$.

Table 2. ^7Li MAS NMR Shifts and Relative Intensities of Tetrahedral and Octahedral Sites in $Li_4Ti_5O_{12}$ and $Li_{5.9}Ti_5O_{12}$

	δ_{tetra} (ppm)	$intensity_{tetra}$	δ_{octa} (ppm)	$intensity_{octa}$
$Li_4Ti_5O_{12}$	0	76.0%	−1.1	24.0%
$Li_{5.9}Ti_5O_{12}$	0	69.2%	−1.0	30.8%

the reliability of the Li distribution on tetrahedral and octahedral sites derived from neutron diffractograms.

Further confirmation of the proposed insertion mechanism can be provided by Raman spectroscopy. Raman spectra of $Li_4Ti_5O_{12}$ and $Li_{5.9}Ti_5O_{12}$ are shown in Figure 5. The spectrum of the $Li_4Ti_5O_{12}$ sample shows the five characteristic allowed lines at 246, 274, 360, 429, and 680 cm^{-1} that are very close to those previously reported.[17,18] The five Raman-allowed phonon peaks are a feature of the spinel structure ($A_{1g} + E_g + 3F_{2u}$).[19] $Li_{5.9}Ti_5O_{12}$ also shows five main lines at 236, 352, 412, 494, and 674 cm^{-1}. In contrast, the frequencies reported for the $LiTi_2O_4$ spinel[20] were 200, 339, 429, 494, and 628 cm^{-1}. The Raman spectra of the chemically Li-inserted $Li_{5.9}Ti_5O_{12}$ shows an overall broadening of the lines, and a new line is observed at 494 cm^{-1} which may be due to coupling of modes involving Li atoms differently bonded in the structure of $Li_{5.9}Ti_5O_{12}$.

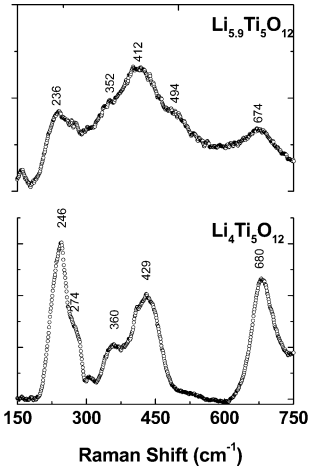

Figure 5. Raman spectra of both $Li_4Ti_5O_{12}$ and chemically inserted $Li_{5.9}Ti_5O_{12}$.

In lithium titanate, the frequencies in the 700−550 cm^{-1} region are known[21] to be ascribable to Ti−O stretches in "TiO_6" octahedra. In oxides where Li is located in "LiO_4" tetrahedral, the frequencies of the Li−O stretches are known to lie within the 400−550 cm^{-1} range.

Discussion

Our X-ray diffraction patterns effectively show that differences are not significant before and after chemical or electrochemical Li-insertion. A simulation of the X-ray diffraction patterns of the spinel $(Li)_{8a}[Li_{0.33}Ti_{1.66}]_{16d}O_4$ and the rocksalt lattice $[Li_2]_{16c}[Li_{0.33}Ti_{1.66}]_{16d}O_4$, not presented here, shows that both structures give a quite similar diffraction pattern with identical peak positions and only minor differences in some peak intensities because of the small diffusion length of Li atom. In contrast to this, neutron diffraction is well suited to clearly distinguish between both phases, as shown in Figure 3. The intensities of several diffraction peaks are clearly different for the two phases. An analysis of the neutron diffraction patterns obtained for the spinel phase before and after chemical Li-insertion showed that no phase transition occurs in this case. Furthermore, the analysis of the peak intensities by the Rietveld method showed that lithium has been inserted not only on octahedral (16c) (like in the spinel to rocksalt

(17) Lutz, H. D. *Z. Naturforsch.* **1969**, *A24*, 1417.
(18) Lutz, H. D.; Muller, B.; Steiner, H. J. *J. Solid State Chem.* **1991**, *90*, 54.
(19) Liu, D. Z.; Hayes, W.; Kurmoo, M.; Dalton, M.; Chen, C. *Physica C* **1994**, *235−240*, 1203.
(20) Gupta, H. C.; Ashdmir, P. *Physica B* **1997**, *233*, 213.
(21) Nakazawa, T. *Nucl. Instrum. Methods Phys. Res.* **2003**, *B206*, 166.

Table 3. Short-Range Force Constants and Interaction between Atoms

	$LiTi_2O_4$	$Li_4Ti_5O_{12}$	$Li_{5.9}Ti_5O_{12}$
α_1 (Li−O)	79 (*80*)[b]	138	151
α_2 (Ti−O) (N/m)	134 (*135*)[b]	132	121
α_3 (O−O)	20[a] (*20*)[b]	20[a]	20[a]
$\nu(A_{1g})$	628 (*628.3*)[d]	675 (*674.6*)[c]	674 (*676.2*)[c]
$\nu(E_g)$	429 (*429.1*)[c]	427 (*426.7*)[c]	412 (*412.8*)[c]
$\nu(F_{2g})$	200	246	236
$\nu(F_{2g})$	339	274	352
$\nu(F_{2g})$	494	360	494

[a] α_3 fixed to 20 N/m as is often observed for oxide spinels. [b] Values from ref 20. [c] Observed Raman lines for samples under study and calculated lines for A_{1g} and E_g modes from sets of α_i's.

phase transition) but also on the tetrahedral sites (48f) of the spinel lattice (insertion in vacant sites of the spinel structure). ^{6}Li MAS NMR has confirmed this result. The tetrahedral contribution $Li_{tetra}/Li_{total} = 75\%$ to the spectrum for the white sample is in good agreement with the expected values for a $Li_4Ti_5O_{12}$ composition if the usual $(Li)_{8a}[Li_{0.33}Ti_{1.66}]_{16d}O_4$ cation distribution[2] is assumed. For the black lithiated sample, the Li_{tetra}/Li_{total} ratio was 70.2% from Rietveld analysis of neutron diffraction data. This value is very close to that obtained from the relative intensities of the signals in the NMR spectra (69.2%), as was previously exposed.

Concerning the analysis of the Raman data, we have not used the angular force constants as was previously done for other spinel containing S and Se.[22] Hence, the dynamical matrix is simplified giving analytical expressions for A_{1g} and E_g modes as follows: $m_0\omega^2(A_{1g}) = \alpha_1 + \alpha_2 + 8\alpha_3$ and $m_0\omega^2(E_g) = \alpha_2 + 2\alpha_3$.[20] Sets of α_i values included in Table 3 give a good agreement between observed and calculated Raman lines for $LiTi_2O_4$, $Li_4Ti_5O_{12}$, and $Li_{5.9}Ti_5O_{12}$. The values of α_1, which is the force constant of the Li−O bond, increase with the Li/O ratio and with the Li amount involved in octahedral sites of the spinel structure from 79 to 151 N/m. On the other hand, α_2, which is the force constant of the Ti−O bond, decreases from 134 to 121 N/m. Variation of α_1 is in agreement with an increase of the Li−O bond strength with an occupation of the tetrahedral sites in $Li_{5.9}Ti_5O_{12}$. Variations of α_2 explain the decreasing apparent value for Ti−O bonds due to Li atoms involved in tetrahedral sites and to the presence of the Ti^{3+} oxidation state leading to a weakest Ti−O bond.

Comparison of the electrochemical behavior of the chemically and the electrochemically inserted sample allows us to conclude that both procedures involve two different insertion mechanisms. Chemical insertion turned out to be irreversible. Lithium cannot be extracted from the chemically inserted sample during an electrochemical test. In contrast to this, the electrochemical insertion in the pristine $Li_4Ti_5O_{12}$ is highly reversible. It is therefore concluded that lithium-insertion on tetrahedral sites, as it occurs in chemical insertion, suppresses the spinel to rocksalt phase transition. Moreover, the preservation of the initial spinel structure is responsible for the irreversibility of the insertion process. It is further concluded that electrochemically inserted lithium occupies exclusively octahedral sites, leading to the desired reversible spinel to rocksalt phase transition.

From all of the characterization techniques used in this work, we found that the chemical Li-insertion process can be summarized by the following reaction:

$$(Li)_{8a}[Li_{0.33}Ti_{1.66}]_{16d}O_4\ \text{(spinel)} + 0.59Li \rightarrow (Li_{0.71})_{8a}(Li_{0.64})_{48f}[Li_{0.24}]_{16c}[Li_{0.33}Ti_{1.66}]_{16d}O_4\ \text{(inserted spinel structure)}$$

and that the electrochemical Li-insertion process can be summarized by the following reaction:

$$(Li)_{8a}[Li_{0.33}Ti_{1.66}]_{16d}O_4\ \text{(spinel)} + 1Li \rightarrow [Li_2]_{16c}[Li_{0.33}Ti_{1.66}]_{16d}O_4\ \text{(rocksalt structure)}$$

Conclusion

In this study, we have shown that the spinel to rocksalt transition does not occur in the chemically inserted phase. XRD and neutron diffraction permit us to propose a structural model in agreement with other experimental investigations such as ^{6,7}Li MAS NMR and Raman spectroscopy. A simple model has been proposed to determine sets of force constants whose variations have been explained in terms of increasing Li−O bonds and Ti^{3+} oxidation state. From an electrochemical point of view, the distorted tetrahedral 48f sites play the role of a trap for Li atoms that are kept in the structure upon insertion or extraction process. Hence, the fractional occupancy of 48f sites may be at the origin of the limitation of the reversible insertion/extraction of Li in the spinel structure.

Acknowledgment. We are greatly indebted to the NEGELiA Project (# ENK6-CT2000-00082) and SAFT society for financial support. J.I.C., J.L.T., and C.P.V. are grateful to CICYT (contract MAT2002-00434). We thank the ILL (Grenoble, France) for neutron diffraction facilities and especially O. Isnard for data collection.

CM0488837

(22) Gupta, H. C.; Parashar, A.; Gupta, V. B.; Tripathi, B. B. *Phys. Status Solidi B* **1990**, *160*, K19.